

A general framework with two Higgs doublets and suppressed FCNC ¹

Gorazd Cvetič ²

Inst. für Physik, Universität Dortmund, 44221 Dortmund, Germany

ABSTRACT

We investigated a general framework of the Standard Model with two Higgs doublets (2HDSM) with suppressed flavor-changing neutral currents (FCNC's). Loop-induced FCNC (and CP-violating) effects, when confronted with experimental constraints for the $K-\bar{K}$, $B-\bar{B}$ and $D-\bar{D}$ mixing and for the $(b \rightarrow s\gamma)$ decay, provide us with constraints on the values of the dominant Yukawa couplings of the charged Higgs, i.e., the values of the couplings of H^\pm to t and b quarks. Once these *low* energy experimental data relevant for the mixings and for the mentioned decay, as well as the theoretical uncertainties for the hadronic matrix elements, are sufficiently reduced, such analyses may be able to rule out the minimal SM and even certain special types of the 2HDSM's (e.g., the popular "type II", and "type I" 2HDSM). In such a case, a more general 2HDSM framework discussed here could still survive as a viable framework. Eventual detection of the charged Higgs in high energy experiments and the measurement of its mass would represent important information that would additionally help to rule out or to favor the various specific 2HDSM scenarios that are contained in the discussed 2HDSM framework.

¹partly based on talk presented at Workshop on Electroweak Symmetry Breaking, Budapest, July 11-13, 1994

²e-mail address: cvetic@het.physik.uni-dortmund.de

1.) Introduction

Experiments show that flavor-changing neutral currents (FCNC) are in nature (at low energies) very suppressed

$$\begin{aligned} Br(K_L^0 \rightarrow \mu^+ \mu^-) &\simeq (7.4 \pm 0.4) \cdot 10^{-9} , & |m_{B_H^0} - m_{B_L^0}| &\simeq (3.36 \pm 0.40) \cdot 10^{-10} MeV , \\ |m_{K_L} - m_{K_S}| &\simeq (3.510 \pm 0.018) \cdot 10^{-12} MeV , & |m_{D_1^0} - m_{D_2^0}| &< 1.32 \cdot 10^{-10} MeV , \\ Br(b \rightarrow s \gamma) &= (2.32 \pm 0.67) \cdot 10^{-4} \text{ etc.} \end{aligned}$$

The various alternative models of electroweak interactions - extensions of the minimal Standard Model (MSM) - must take into account the FCNC suppression. The most conservative extensions of the MSM are apparently the models with two Higgs doublets (2HDSM's).

The conditions for the one-loop FCNC suppression of contributions coming from gauge boson loops, i.e., the allowed representations of fermions, have been investigated some time ago [1]. In addition, Glashow and Weinberg [1] proposed for the Higgs sector the MSM (one Higgs doublet model) and the “type I” and “type II” 2HDSM's. They proposed them as models which, in a “natural” way, have the zero value for the flavor-changing renormalized Yukawa couplings in the neutral sector (called from now on: FCN renormalized Yukawa couplings). These two types of the 2HDSM's have been widely discussed in the literature. Their Yukawa sector Lagrangians with bare or renormalized quantities have the form:

a) “type I” [2HDSM(I)] - just one Higgs doublet (say, $H^{(1)}$) couples to fermions

$$\mathcal{L}_{\text{Yukawa}}^{(I)} = - \sum_{i,j=1}^3 \{ \tilde{D}_{ij}^{(q)} (\bar{q}_L^{(i)} H^{(1)}) d_R^{(j)} + \tilde{U}_{ij}^{(q)} (\bar{q}_L^{(i)} \tilde{H}^{(1)}) u_R^{(j)} + \text{h.c.} \} + \dots , \quad (1)$$

where the dots represent the terms for the leptons. The following notations are used:

$$H = \begin{pmatrix} H^+ \\ H^0 \end{pmatrix} , \quad \tilde{H} = i\tau_2 H^* , \quad q^{(i)} = \begin{pmatrix} u^{(i)} \\ d^{(i)} \end{pmatrix} , \quad q^{(1)} = \begin{pmatrix} u \\ d \end{pmatrix} , \quad q^{(2)} = \begin{pmatrix} c \\ s \end{pmatrix} , \quad q^{(3)} = \begin{pmatrix} t \\ b \end{pmatrix} ,$$

and similarly for the leptonic doublets $\ell^{(i)}$ containing Dirac neutrinos and charged leptons.

This model is very closely related to the minimal SM (MSM), the only difference in the Yukawa sector being the smaller vacuum expectation value $\langle (H^0)^{(1)} \rangle_0 = v_1 / \sqrt{2} < v / \sqrt{2}$ ($v \approx 246.22 GeV$), and hence the correspondingly larger Yukawa coupling parameters.

b) “type II” [2HDSM(II)] - one doublet ($H^{(1)}$) couples to the “down-type” right-handed fermions d_R , ℓ_R^- and is responsible for the “down-type” masses; the other doublet ($H^{(2)}$) couples to the “up-type” fermions u_R , ν_R and is responsible for their masses:

$$\mathcal{L}_{\text{Yukawa}}^{(II)} = - \sum_{i,j=1}^3 \{ \tilde{D}_{ij}^{(q)} (\bar{q}_L^{(i)} H^{(1)}) d_R^{(j)} + \tilde{U}_{ij}^{(q)} (\bar{q}_L^{(i)} \tilde{H}^{(2)}) u_R^{(j)} + \text{h.c.} \} + \dots . \quad (2)$$

The mass matrices are proportional to the vacuum expectation values (VEV's) of the Higgses: $M_u^{(q,\ell)} = v_2 \tilde{U}^{(q,\ell)} / \sqrt{2}$, $M_d^{(q,\ell)} = v_1 \tilde{D}^{(q,\ell)} / \sqrt{2}$, where

$$\langle H^{(2)} \rangle_0 = \frac{e^{i\xi}}{\sqrt{2}} \begin{pmatrix} 0 \\ v_2 \end{pmatrix} , \quad \langle H^{(1)} \rangle_0 = \frac{1}{\sqrt{2}} \begin{pmatrix} 0 \\ v_1 \end{pmatrix} , \quad v_1^2 + v_2^2 = v^2 (\approx 246^2 GeV^2) .$$

The phase ξ between the two VEV's, if it is nonzero, is responsible for CP violation in the scalar and in the Yukawa sector. The expressions are written in any $SU(2)_L$ -basis, i.e., a basis in which $q_L^{(i)}$ and $\ell_L^{(i)}$ are $SU(2)_L$ -isodoublets.

Later on, extensions with more than one Higgs doublet other than the 2HDSM(I) and (II) have been proposed. They usually satisfy either one of the following conditions:

- (a) the renormalized FCN Yukawa couplings are *zero*, and the loop-induced FCNC phenomena are sufficiently suppressed [2]; these models possess an exact family (“horizontal”) symmetry which ensures that both the bare and the renormalized FCN Yukawa couplings are zero simultaneously (in the formal limit of the infinite UV cut-off).
- (b) FCN renormalized Yukawa couplings are nonzero, but small; the suppression of these FCN Yukawa couplings is brought about by an additional mechanism, e.g., by approximate family symmetries [3, 4]; the FCN bare Yukawa couplings are not necessarily small.

On the other hand, we are going to consider several phenomenological consequences of the following 2HDSM framework: within the framework, the renormalized FCN Yukawa couplings are either zero or they are “sufficiently” suppressed. By “sufficiently” we mean that their suppression is such that the leading 1-particle-irreducible (1PI) loop-induced contributions to the considered FCNC processes and phenomena (particularly the box diagrams for the B - \bar{B} and D - \bar{D} mixing) dominate over the direct tree level contributions of the renormalized FCN Yukawa couplings³. At the end of Section 4, we will estimate the upper bounds on the relevant renormalized FCN Yukawa couplings satisfying the condition of the “sufficient” suppression. Physically, the considered framework includes models of type (a) and a subset of the models of type (b). From the algebraic point of view, the considered framework, although without imposed family symmetries, is of type (a), because we will neglect the effects of the renormalized FCN Yukawa couplings. In addition, for simplicity, we assume that the CP-violating phase ξ between the two VEV’s is so small that its effects will be neglected (by setting $\xi = 0$). The CP violation then originates solely from the δ angle of the Cabbibo-Kobayashi-Maskawa (CKM) mixing matrix. The renormalized Yukawa interactions in this framework, in any $SU(2)_L$ -basis, have at first glance the most general form

$$\begin{aligned} \mathcal{L}_Y = & - \sum_{i,j=1}^3 \left\{ \tilde{D}_{ij}^{(1)} (\bar{q}_L^{(i)} H^{(1)}) d_R^{(j)} + \tilde{D}_{ij}^{(2)} (\bar{q}_L^{(i)} H^{(2)}) d_R^{(j)} + \right. \\ & \left. + \tilde{U}_{ij}^{(1)} (\bar{q}_L^{(i)} \tilde{H}^{(1)}) u_R^{(j)} + \tilde{U}_{ij}^{(2)} (\bar{q}_L^{(i)} \tilde{H}^{(2)}) u_R^{(j)} + h.c. \right\} + \{ \bar{\ell} H \ell \text{-terms} \} . \end{aligned} \quad (3)$$

The quarks are here in an arbitrary $SU(2)_L$ -basis (not in the mass basis). The renormalized 3×3 -Yukawa matrices $\tilde{D}^{(1)}$, $\tilde{D}^{(2)}$, $\tilde{U}^{(1)}$ and $\tilde{U}^{(2)}$ are in the present framework such that in the mass basis of quarks they become all *simultaneously* diagonal, in order to have zero (or: negligible) FCN Yukawa couplings. By that we mean that \mathcal{L}_Y in the mass basis of quarks has the following form:

$$\begin{aligned} \mathcal{L}_Y = & - \sum_{i,j=1}^3 \left\{ \bar{u}_L^{(i)} \left[H^{(1)+} (VD^{(1)})_{ij} + H^{(2)+} (VD^{(2)})_{ij} \right] d_R^{(j)} + \bar{d}_L^{(i)} \left[H^{(1)0} D_{ij}^{(1)} + H^{(2)0} D_{ij}^{(2)} \right] d_R^{(j)} \right. \\ & \left. + \bar{u}_L^{(i)} \left[(H^{(1)0})^* U_{ij}^{(1)} + (H^{(2)0})^* U_{ij}^{(2)} \right] u_R^{(j)} + \bar{d}_L^{(i)} \left[-H^{(1)-} (V^\dagger U^{(1)})_{ij} - H^{(2)-} (V^\dagger U^{(2)})_{ij} \right] u_R^{(j)} \right. \\ & \left. + h.c. \right\} , \end{aligned} \quad (4)$$

$$\text{where: } \quad H^{(k)} = \begin{pmatrix} H^{(k)+} \\ H^{(k)0} \end{pmatrix}, \quad \tilde{H}^{(k)} = i\tau_2 (H^{(k)})^* = \begin{pmatrix} (H^{(k)0})^* \\ -H^{(k)-} \end{pmatrix}, \quad (k = 1, 2) .$$

³ The tree level contributions of the renormalized couplings are in general tree level contributions of the bare couplings plus (cut-off dependent parts of the) 1-particle-reducible (1PR) loop corrections calculated with these bare couplings.

In formula (3), the quarks are in the mass basis, V is the usual (complex) CKM matrix, and $U^{(1)}$, $U^{(2)}$, $D^{(1)}$ and $D^{(2)}$ are the diagonal renormalized Yukawa matrices (in the mass basis), i.e., the FCN Yukawa couplings are all zero. Furthermore, these matrices are all real, because we assume that all the CP violation is of the CKM-type only ($\xi = 0$) and can therefore be presented with a single δ -angle in the complex CKM matrix. We note that “type I” and “type II” models (eqs. (1) and (2)) are special cases (subsets) of this framework. In (3) we omitted the leptonic sector.

There may be objections against such a 2HDSM framework, on the grounds that, unlike the 2HDSM(I) and (II), it has no discrete or continuous family (“horizontal”) symmetries. These family symmetries would impose in a “natural” way the value zero on the bare FCN Yukawa couplings, and would keep these Yukawa couplings at the value zero even when they are formally renormalized from $\Lambda = \infty$ to low energies⁴. It is true that the renormalized FCN Yukawa couplings in (3) acquire the value zero (in the mass basis) not in a “natural” way, but only as a consequence of an algebraic condition on the renormalized Yukawa couplings - the condition that $U^{(1)}$, $U^{(2)}$, $D^{(1)}$ and $D^{(2)}$ all be diagonal. In general, such a condition leads to the following behavior of the FCN Yukawa couplings: at low energies of probes, i.e., when they are renormalized, they are (negligibly) small; only as the energy of probes is increased, they may in general grow, as dictated by the renormalization group equations (RGE’s). In the formal limit of $E_{\text{probes}} (= \Lambda) = \infty$, the resulting bare FCN Yukawa couplings may in general diverge. In view of this, the objection against the framework can be countered in at least two different ways:

- Since the FCNC suppression is an essentially low energy phenomenon ($E_{\text{probes}} \lesssim 100 \text{ GeV}$), there is no absolutely compelling reason for it to remain in force when the energy of probes is increased beyond the present experimentally accessible regions and relevant phenomena and processes are investigated at such an energy. Then, the (negligibly) small values of the FCN Yukawa couplings at low energies could be ensured by some as yet unknown mechanism (which is definitely other than exact family symmetries), e.g., by an approximate family symmetry (cf. Refs. [3, 4]), or could be simply accidental.
- Even if we assume the “naturalness” of the FCNC’s, i.e., that the suppression of the FCN Yukawa couplings to zero remains in force even at increasing E_{probes} because ensured by certain assumed exact family symmetries, we can regard the considered framework (3) as a framework containing the union of all such “natural” 2HDSM’s. Even in such a case, the phenomenological analysis of the framework (3) would carry relevance, because such an analysis does not investigate theoretical constraints of a specific model, but only phenomenological constraints in a rather broad framework.

In Section 2 we discuss the charged sector of the Yukawa couplings in the proposed 2HDSM framework. In Section 3 we investigate phenomenological constraints on this sector which are imposed by the $K-\bar{K}$ and $B-\bar{B}$ mixing data. In Sections 4 and 5 we investigate the constraints on this sector which come from the $D-\bar{D}$ mixing and from the $(b \rightarrow s\gamma)$ decay data, respectively. The conclusions are summarized in Section 6.

⁴ In the 2HDSM(II), the family symmetry in \mathcal{L}_Y is of U(1)-type: $d_R^{(j)} \rightarrow e^{i\alpha} d_R^{(j)}$, $H^{(1)} \rightarrow e^{-i\alpha} H^{(1)}$ ($j=1,2,3$), the other fields remaining unchanged. This symmetry ensures that, in the course of renormalization, no loop-induced ($\ln \Lambda$ cut-off dependent) Yukawa couplings other than those of the form (2) can appear. In the 2HDSM(I), the family symmetry is similar: $d_R^{(j)} \rightarrow e^{i\alpha} d_R^{(j)}$, $u_R^{(j)} \rightarrow e^{-i\alpha} u_R^{(j)}$, $H^{(1)} \rightarrow e^{-i\alpha} H^{(1)}$.

2.) The Yukawa sector of the charged Higgs in a general 2HDSM framework

The charged-current part of the quarks corresponding to the Lagrangian (3) can be deduced in a straightforward manner

$$\mathcal{L}_Y^{cc} = H^{(+)}[-\bar{u}_L V D d_R + \bar{u}_R U V d_L] + H^{(-)}[-\bar{d}_R D V^\dagger u_L + \bar{d}_L V^\dagger U u_R] . \quad (5)$$

This expression is in the unitary gauge and in the physical bases of the quarks *and* of the charged Higgses $H^{(\pm)}$. V is the usual (complex) CKM matrix, $u^T = (u, c, t)$, $d^T = (d, s, b)$; U and D are specific linear combinations of the real diagonal Yukawa matrices $U^{(j)}$ and $D^{(j)}$

$$U = -\sin \beta U^{(1)} + \cos \beta U^{(2)} , \quad D = -\sin \beta D^{(1)} + \cos \beta D^{(2)} , \quad (6)$$

where $\tan \beta$ is the ratio of the absolute values of the VEV's ($\tan \beta = v_2/v_1$), and the mass basis is used. U and D are diagonal and real ($\xi = 0$). On the other hand, the (diagonal) mass matrices of quarks are obtained from the corresponding orthonormal linear combinations

$$\frac{\sqrt{2}}{v} M_u = \cos \beta U^{(1)} + \sin \beta U^{(2)} , \quad \frac{\sqrt{2}}{v} M_d = \cos \beta D^{(1)} + \sin \beta D^{(2)} . \quad (7)$$

Therefore, if we assume that no peculiar cancelations occur, we have the following hierarchy:

$$\frac{U_{ii}}{U_{jj}} \sim \frac{m_u^{(i)}}{m_u^{(j)}} , \quad \frac{D_{ii}}{D_{jj}} \sim \frac{m_d^{(i)}}{m_d^{(j)}} \quad (i, j = 1, 2, 3) . \quad (8)$$

In such a case, the coupling U_{33} of the charged Higgs $H^{(+)}$ to $\bar{t}_R b_L$ and the coupling ($-D_{33}$) of $H^{(+)}$ to $\bar{t}_L b_R$ are the two dominant Yukawa couplings in the charged sector. We will assume in the rest of the presentation that this is the case, i.e., that the hierarchy (8) holds. Stated otherwise, the sector of the Yukawa couplings of charged Higgs to quarks provides us, within the present framework, with only two additional real “normalized” parameters

$$X^{(U)}(E) = \frac{U_{33}(E)v}{m_t(E)\sqrt{2}} , \quad X^{(D)}(E) = -\frac{D_{33}(E)v}{m_b(E)\sqrt{2}} , \quad (9)$$

where E is a typical energy of probes which depends on the process considered⁵. 2HDSM(I) and (II) [cf. Eqs. (1),(2)] are just two special cases of the present framework, and $X^{(U)}$ and $X^{(D)}$ are in these cases independent of E :

$$\text{2HDSM(I):} \quad U^{(1)} = D^{(1)} = 0 \quad X^{(U)}(E) = -X^{(D)}(E) = \cot \beta . \quad (10)$$

$$\text{2HDSM(II):} \quad U^{(1)} = D^{(2)} = 0 , \quad X^{(U)}(E) = 1/X^{(D)}(E) = \cot \beta . \quad (11)$$

Therefore, if abandoning the present general framework in favor of the 2HDSM(I) or (II), the two parameters $X^{(U)}$ and $X^{(D)}$ would not be free any more, but would be completely fixed by the VEV's (i.e., by $\tan \beta$) and would be interrelated.

In the analysis below, we will search for constraints on these two additional parameters $X^{(U)}$ and $X^{(D)}$. The constraints will be dictated by the experimental data on various

⁵ Formally, E is the finite upper energy cut-off used in the renormalized Lagrangians (3)-(5). Later we will argue that this energy E , for the quantities $U_{33}(E)$ and $D_{33}(E)$ (or $X^{(U)}(E)$ and $X^{(D)}(E)$) appearing in one-loop formulas for specific processes, is approximately equal to the higher of the two momenta (or masses) of the two quark legs at the vertex U_{33} or D_{33} . This energy turns out to be $E \simeq m_t$ for the B - \bar{B} and K - \bar{K} mixing and for the $(b \rightarrow s\gamma)$ decay, and $E \simeq m_b$ for the D - \bar{D} mixing.

meson-antimeson mixings and the ($b \rightarrow s\gamma$) decay. In principle, these essentially *low* energy phenomena alone could at some future point, when experimental and theoretical uncertainties are reduced, give us a possibility to rule out the MSM, or even to rule out 2HDSM(II) and (I). In the latter case, the constraint $X^{(U)} \cdot X^{(D)} = 1$ and/or the constraint $X^{(U)} = -X^{(D)}$ would have to be abandoned in favor of a more general framework, e.g. the 2HDSM framework discussed here. For the special cases 2HDSM(II) and (I), phenomenological constraints have been investigated by several authors [5]. Here they will be studied within the presented more general framework. However, before doing this, we note that certain constraints on $X^{(U)}$ and $X^{(D)}$ can be immediately obtained by demanding that the theory behave perturbatively. This demand can be implemented approximately, by requiring that the relevant Yukawa couplings $U_{33}(1 \pm \gamma_5)/2$ and $D_{33}(1 \pm \gamma_5)/2$ of the charged Higgs to b and t quarks [cf. Eq. (5)] not exceed the QCD coupling $g_s^2(M_W^2) (= 4\pi\alpha_s(M_W^2) \simeq 1.5)$

$$\frac{D_{33}(m_b)}{2}, \frac{D_{33}(m_t)}{2}, \frac{U_{33}(m_t)}{2} \lesssim 1.5 \Rightarrow |X^{(D)}(m_b)| \lesssim 120, |X^{(D)}(m_t)| \lesssim 190, |X^{(U)}(m_t)| \lesssim 3.0 . \quad (12)$$

3.) B - \bar{B} and K - \bar{K} mixing in a general 2HDSM framework

Since the $H^{(\pm)}$ -exchanges influence the short distance contributions to the B_d^0 - \bar{B}_d^0 and K^0 - \bar{K}^0 mixing, the experimental values of $|m_{B_H^0} - m_{B_L^0}|$, and of the K^0 - \bar{K}^0 CP-violating parameter ε_K would provide us with restrictions on the (dominant) $X^{(U)}$ coupling strength of $H^{(\pm)}$ to quarks. These parameters are dominated by short distance physics, because it is mostly the very heavy top quark that dominates over the other quark contributions in the relevant electroweak loop diagrams. The dominant one-loop electroweak diagrams contributing to these mass differences are the W-W, H-W and H-H exchange box diagrams of Fig. 1. The resulting effective four-fermion couplings are

$$\begin{aligned} \mathcal{L}_{eff} (= \mathcal{L}_{eff}^{WW} + \mathcal{L}_{eff}^{HW} + \mathcal{L}_{eff}^{HH}) &\simeq \mathcal{A}^K \left[\overline{d(x)^a} \gamma^\mu \left(\frac{1 - \gamma_5}{2} \right) s(x)^a \right]^2 \quad (\text{for } \bar{K}^0 \rightarrow K^0) \\ &\simeq \mathcal{A}^B \left[\overline{b(x)^a} \gamma^\mu \left(\frac{1 - \gamma_5}{2} \right) d(x)^a \right]^2 \quad (\text{for } B_d^0 \rightarrow \bar{B}_d^0) , \end{aligned} \quad (13)$$

where \mathcal{A}^K and \mathcal{A}^B are the corresponding box amplitudes from Fig. 1

$$\mathcal{A} = \mathcal{A}_{WW} + \mathcal{A}_{HW} + \mathcal{A}_{HH} .$$

The general formulas for these electroweak amplitudes, within the present framework, can be calculated in a straightforward way, if we ignore the masses and momenta of the external quark legs

$$\mathcal{A}_{WW} = \frac{G_F^2 M_W^2}{4\pi^2} \sum_{k,n=2}^3 \zeta_k \zeta_n \mathcal{E}(x_k, x_n) , \quad \mathcal{A}_{HH} = -\frac{1}{128\pi^2 M_{H^\pm}^2} \sum_{k,n=1}^3 \zeta_k \zeta_n U_{kk}^2 U_{nn}^2 \mathcal{I}(y_k, y_n) . \quad (14)$$

$$\mathcal{A}_{HW} = -\frac{G_F}{4\sqrt{2}\pi^2} \sum_{k,n=1}^3 \zeta_k \zeta_n \sqrt{x_k x_n} U_{kk} U_{nn} \mathcal{J}(x_k, x_n, x_h) , \quad (15)$$

We denoted here $x_k = (m_k^{(u)}/M_W)^2$, $y_k = (m_k^{(u)}/M_{H^\pm})^2$ ($k = 1, 2, 3$), $x_h = (M_{H^\pm}/M_W)^2$; ζ_k are the CKM-mixing factors

$$\zeta_3 = \zeta_t = V_{td}^* V_{ts} \quad (\text{for } \bar{K}^0 \rightarrow K^0) , \quad \zeta_3 = \zeta_t = V_{td} V_{tb}^* \quad (\text{for } B^0 \rightarrow \bar{B}^0) , \quad (16)$$

and analogously for ζ_2 and ζ_1 . The integrals \mathcal{E} , \mathcal{J} and \mathcal{I} are dimensionless and tame functions of the masses of internal particles

$$\begin{aligned}\mathcal{J}(x_k, x_n; x_h) &= \int_0^\infty \frac{dz z(1+z/4)}{(z+1)(z+x_h)(z+x_k)(z+x_n)}, \\ \mathcal{I}(y_k, y_n) &= \int_0^\infty \frac{dz z^2}{(z+1)^2(z+y_k)(z+y_n)}.\end{aligned}\quad (17)$$

$\mathcal{E}(x_k, x_n)$ is a well known Inami-Lim function [6]. The integration variable z in the above expressions for \mathcal{J} and \mathcal{I} is equal to \bar{p}^2/M_W^2 and $\bar{p}^2/M_{H^\pm}^2$, respectively, \bar{p} being the Euclidean version of the 4-momentum of the loop. In view of the previous discussion, we will neglect in the above expressions for \mathcal{A}_{HW} and \mathcal{A}_{HH} all the terms containing U_{11} and U_{22} . Therefore, \mathcal{A}_{HW} and \mathcal{A}_{HH} contain each just one term, namely the term proportional to $\zeta_t^2 x_t U_{33}^2$ and to $\zeta_t^2 U_{33}^4$, respectively. In the above expression for \mathcal{L}_{eff}^{HH} , we ignored several other induced four-fermion terms, e.g. terms of the type $[\overline{b(x)}]^a \left(\frac{1-\gamma_5}{2}\right) d(x)^a]^2$. It turns out that the dimensionless integrals appearing in the amplitudes at such terms are roughly an order of magnitude smaller than the integrals \mathcal{I} and \mathcal{J} in eqs. (17). Furthermore, the dominant coupling strengths at such terms are proportional to $\zeta_t^2 U_{33}^2 D_{22}^2$ for $K^0-\bar{K}^0$, and to $\zeta_t^2 U_{33}^2 D_{33}^2$ for $B_d^0-\bar{B}_d^0$. Neglecting such terms is justifiable if $|D_{33}| \lesssim |U_{33}|$ (at $E \simeq m_t$), i.e., if $|X^D| \lesssim 60 \cdot |X^{(U)}|$ (in 2HDSM(II), this condition reads: $\tan \beta \lesssim 8$)⁶. We will see in the analysis of the $(b \rightarrow s\gamma)$ decay that this condition is satisfied in most of the region in the plane $X^{(D)}$ vs $X^{(U)}$ allowed by this decay.

The next step is to include in the above formulas the QCD corrections in the leading logarithmic approximation. Many authors have investigated these corrections for the box exchange diagrams in the MSM ([7, 8, 9, 10] and references therein)⁷. Applying the approach of [8] to the W-H and H-H box exchange diagrams (which contain two top quark propagators), we arrive at the following leading QCD correction factors to the integrands of (17):

- (a):** The leading-log summation for the exchange of gluons between the external quark legs of the same flavor (Fig. 2a) yields the factor

$$\left[\frac{\alpha_s(p^2)}{\alpha_s(\mu^2)} \right]^{2/b_{\text{nf}}} \quad (b_{\text{nf}} = 11 - \frac{2}{3}n_{\text{f}}). \quad (18)$$

Here, p^2 is the 4-momentum of the electroweak loop (to be integrated over), n_{f} is the effective number of flavors at this energy ($n_{\text{f}} \simeq 5$ for $|p^2| < m_t^2$, $n_{\text{f}} \simeq 6$ for $|p^2| > m_t^2$), and μ is the lower (infrared) energy cut-off which is roughly to be identified with the momenta of the quark constituents of the meson. We will take $\mu = m_b \approx 4.9\text{GeV}$ ($\Rightarrow \alpha_s(\mu^2) \approx 0.21$) for $B_d^0-\bar{B}_d^0$ mixing, as suggested by Buras *et al.* [10], and $\alpha_s(\mu^2) \approx 1$ for $K^0-\bar{K}^0$ mixing, as suggested by several authors [7, 8].

- (b):** The effects of the “running” top mass $m_t(p^2)$ and the “running” Yukawa couplings $U_{33}(p^2)$ (cf. Figs. 2b,c) yield the factor

$$\left[\frac{\alpha_s(p^2)}{\alpha_s(m_t^2)} \right]^{16/b_{\text{nf}}}. \quad (19)$$

⁶ We assumed here $m_t^{\text{phy}} = 175\text{GeV}$ and $m_b^{\text{phy}} = 4.9\text{GeV}$, which corresponds to $m_t(m_t) \simeq 167\text{GeV}$ and $m_b(m_t) \simeq 2.77\text{GeV}$.

⁷ The authors of [10] have calculated even the next-to-leading order QCD corrections in an apparently consistent way.

(c): The effects of the gluon exchange between an outer leg and the internal (top quark) propagator (cf. Fig. 2d) do not contribute appreciably, because the top quark is so heavy. We can intuitively explain this by imagining that the top quark is so heavy as to have no propagator, i.e., the propagator shrinks to a point, and the gluon has “no place” to land on it. This argument holds as long as M_{H^\pm} is not exceedingly high (i.e., as long as $M_{H^\pm} \sim m_t$).

It turns out that the factor in (b) is rather close to unity for most relevant momenta (as long as $M_{H^\pm} \sim m_t$), and that therefore the factor in (a) is the crucial one numerically. The QCD-corrected integrals of (17) are

$$\mathcal{J}(x_k, x_n; x_h) = \int_0^\infty \frac{dz z(1+z/4)}{(z+1)(z+x_h)(z+x_k)(z+x_n)} \cdot \left[\frac{\alpha_s(zM_W^2)}{\alpha_s(\mu^2)} \right]_{\text{b}_{\text{nf}}}^2 \cdot \left[\frac{\alpha_s(zM_W^2)}{\alpha_s(m_t^2)} \right]_{\text{b}_{\text{nf}}}^{16} \quad (20)$$

$$\mathcal{I}(y_k, y_n) = \int_0^\infty \frac{dz z^2}{(z+1)^2(z+y_k)(z+y_n)} \cdot \left[\frac{\alpha_s(zM_{H^\pm}^2)}{\alpha_s(\mu^2)} \right]_{\text{b}_{\text{nf}}}^2 \cdot \left[\frac{\alpha_s(zM_{H^\pm}^2)}{\alpha_s(m_t^2)} \right]_{\text{b}_{\text{nf}}}^{16} \quad (21)$$

We calculated numerically these integrals, taking for $\alpha_s(p^2)$ the two-loop solution with $\alpha_s(M_Z^2) = 0.117$. The results of the analysis for $B_d^0\text{-}\bar{B}_d^0$ and $K^0\text{-}\bar{K}^0$ mixing depend only very weakly on the precise value of $\alpha_s(M_Z^2)$. Furthermore, we included the leading (known) QCD corrections of the MSM case, i.e., to the W - W exchange box diagrams [7]-[10] (W stands here for the *physical* gauge boson W), by making the following replacements in the amplitude \mathcal{A}_{WW}^K : $\zeta_c^2 \mapsto 0.81\zeta_c^2$, $\zeta_t\zeta_c \mapsto 0.37\zeta_t\zeta_c$; $\zeta_t^2 \mapsto 0.57\zeta_t^2$, and in \mathcal{A}_{WW}^B : $\zeta_t^2 \mapsto 0.86\zeta_t^2$. The replacements for the ζ_t^2 -terms in the cases of both mixings were taken from Ref. [10], where they are substantiated by careful investigation of the next-to-leading QCD corrections in the MSM. We note that it is the ζ_t^2 -terms which contribute the most to the short distance physics in the case of the $K\text{-}\bar{K}$ mixing, and almost exclusively in the case of the $B\text{-}\bar{B}$ mixing.

The correction factor (19), although numerically not important in the integrals (20) and (21), suggests that the relevant scale E ($=\sqrt{p^2}$) to be used in the vertex coupling $U_{33}(E)$, as well as in the mass $m_t(E)$ [in $x_t = (m_t(E)/M_W)^2$ and $y_t = (m_t(E)/M_{H^\pm})^2$ in Eqs. (20) and (21)], is $E \simeq m_t$. More generally, the scale E used in the “running” vertex couplings $U_{33}(E)$ and $D_{33}(E)$ appearing in the one-loop (electroweak) formulas is approximately equal to the mass m_q of the heavier of the two quarks attached to the considered vertex. This is connected to the fact that the largest contribution to the electroweak one-loop integral is for the internal loop momenta in the region $p^2 \sim m_q^2$. This argument appears to be supported by the works [7, 8] (these works suggest the formula (19)) and by the work of Buras *et al.* [10]⁸. By adjusting the “running” energy of probes E in the electroweak formulas in this way appears to take into account some QCD-correction effects which turn out to be quite important in some processes. For example, in the ($b \rightarrow s\gamma$) decay the electroweak formulas contain both $U_{33}(E)$ and $D_{33}(E)$ Yukawa couplings, or equivalently: $X^{(U)}(E)$ and $X^{(D)}(E)$ (see Section 5). Since the relevant electroweak loops are dominated by the top quark contributions (cf. Fig. 4b), we have $E \simeq m_t$. When normalizing $X^{(D)}$ according to (9), we therefore use $m_b(m_t)$ ($\simeq 2.8 \text{ GeV}$) and not $m_b(m_b)$ ($\simeq 4.4 \text{ GeV}$). On the other hand, the charged Higgs contributions to the $D^0\text{-}\bar{D}^0$ mixing are dominated by the box diagrams containing the bottom quarks. Therefore, the formulas there, containing $X^{(D)}(E)$, should have $E \simeq m_b$. All in all, the $B\text{-}\bar{B}$ and $K\text{-}\bar{K}$ mixing will result in constraints on $X^{(U)}(m_t)$, the

⁸ The authors of [10] also argue that the mass $m_t(E)$ in the internal top quark propagators of the electroweak loop [i.e., in $x_t(E)$ and $y_t(E)$ in integrals (20) and (21)] should be taken at $E \approx m_t$.

D - \bar{D} mixing in constraints on $X^{(D)}(m_b)$, and the $(b \rightarrow s\gamma)$ decay in constraints on $X^{(U)}(m_t)$ and $X^{(D)}(m_t)$.

Relations of the resulting amplitudes \mathcal{A}^K and \mathcal{A}^B to the experimental inputs of K and B physics are well known

$$\begin{aligned} \sqrt{2}(\Delta M_{K_L^0 - K_S^0})(|\varepsilon_K| + 0.05 \frac{\varepsilon'_K}{\varepsilon_K}) &\simeq -\frac{1}{2M_{K^0}} \text{Im} \langle K^0 | \mathcal{L}_{eff}(x=0) | \bar{K}^0 \rangle \\ &= -\frac{1}{2M_{K^0}} \text{Im} (\mathcal{A}^K) \cdot \langle K^0 | \left[\bar{d}^a \gamma^\mu \left(\frac{1-\gamma_5}{2} \right) s^a \right]^2 | \bar{K}^0 \rangle \end{aligned} \quad (22)$$

$$M_{B^0} |\Delta M_{B_H^0 - B_L^0}| \simeq |\langle \bar{B}_d^0 | \mathcal{L}_{eff}(x=0) | B_d^0 \rangle| = |\mathcal{A}^B| \cdot \langle \bar{B}_d^0 | \left[\bar{b}^a \gamma^\mu \left(\frac{1-\gamma_5}{2} \right) d^a \right]^2 | B_d^0 \rangle, \quad (23)$$

where we adopt the normalization conventions: $\langle P^0 | P^0 \rangle = Vol \cdot 2M_{P^0}$ ($P^0 = K^0, B^0, \dots$; Vol is the 3-dimensional volume of the space). Perturbative (short distance) contributions in the above relations are represented by the amplitudes $\text{Im}(\mathcal{A}^K)$, \mathcal{A}^B . On the other hand, the hadronic matrix elements $\langle K^0 | \dots | \bar{K}^0 \rangle$ and $\langle \bar{B}_d^0 | \dots | B_d^0 \rangle$ represent the low energy (non-perturbative) effects. Experiments provide us with the following values for the ΔM 's and the CP-violating parameters ε_K and ε'_K [11]:

$$\Delta M_{K_L^0 - K_S^0} = 3.510 \cdot 10^{-15} GeV (1 \pm 5.1 \cdot 10^{-3}), \quad \Delta M_{B_H^0 - B_L^0} = 3.36 \cdot 10^{-13} GeV (1 \pm 0.12), \quad (24)$$

$$|\varepsilon_K| = 2.26 \cdot 10^{-3} (1 \pm 0.037), \quad \frac{\varepsilon'_K}{\varepsilon_K} \simeq 1.5 \cdot 10^{-3}, \quad M_{B_d^0} = 5.279 GeV, \quad M_{K^0} = 0.4977 GeV. \quad (25)$$

Among these parameters, only $\Delta M_{B_H^0 - B_L^0}$ has an appreciable experimental uncertainty (12 percent). For the hadronic matrix elements, we have the following theoretical uncertainties:

$$\langle K^0 | \left[\bar{d}^a \gamma^\mu \left(\frac{1-\gamma_5}{2} \right) s^a \right]^2 | \bar{K}^0 \rangle = \frac{2}{3} F_K^2 B_K M_{K^0}^2, \quad 0.5 \lesssim B_K \lesssim 1.0, \quad (F_K = 160 MeV). \quad (26)$$

$$\langle \bar{B}_d^0 | \left[\bar{b}^a \gamma^\mu \left(\frac{1-\gamma_5}{2} \right) d^a \right]^2 | B_d^0 \rangle = \frac{2}{3} F_B^2 B_B M_{B^0}^2, \quad 0.12 GeV \lesssim F_B \sqrt{B_B} \lesssim 0.25 GeV. \quad (27)$$

We note that the QCD-sum rules and lattice calculations prefer the following values of B_K and $F_B \sqrt{B_B}$:

$$0.6 \lesssim B_K \lesssim 0.9, \quad 0.17 GeV \lesssim F_B \sqrt{B_B} \lesssim 0.22 GeV. \quad (28)$$

In addition, we have many uncertainties also in the CKM matrix V [in \mathcal{L}_Y^c of Eq. (5)] which influence the parameters ζ_j . The Cabbibo angle is fairly well determined ($\sin \theta_{12} = 0.221 \pm 0.003$), so we use the middle value for it. On the other hand, the other two CKM rotation angles θ_{23} and θ_{13} (in the convention of Chau and Keung, or Maiani) have the following uncertainties [11] in the 90 percent confidence limit

$$0.032 < \sin \theta_{23} < 0.048, \quad 0.002 < \sin \theta_{13} < 0.005. \quad (29)$$

All three rotation angles lie in the first quadrant. Furthermore, the CLEO [12] and ARGUS [13] collaborations have measured $b \rightarrow u$ transitions in semileptonic B decays, with the further resulting restriction

$$\frac{\sin \theta_{13}}{\sin \theta_{23}} = \left| \frac{V_{ub}}{V_{cb}} \right| = 0.08 \pm 0.02. \quad (30)$$

On the hand, the fourth angle δ in the CKM matrix, responsible for CP violation, is completely undetermined yet. We note that the restrictions (29) and (30) are mostly obtained

from weak semileptonic decays of relevant quarks and from the requirement of unitarity. E.g., the restrictions on $|V_{cb}|$ ($\simeq \sin \theta_{23}$) are obtained largely from ($b \rightarrow cW^- \rightarrow c\ell^-\bar{\nu}_\ell$) decay; the restrictions on $|V_{ub}|$ ($= \sin \theta_{13}$) are obtained largely from the requirement of unitarity in the first row of the CKM matrix ($|V_{ub}|^2 = 1 - |V_{ud}|^2 - |V_{us}|^2$), the two other elements of this row ($|V_{ud}|$, $|V_{us}|$) being determined largely by the comparison of the nuclear beta decay to muon decay, and by semileptonic decay of K mesons ($K^+ \rightarrow \pi^0 e^+ \nu_e$, $K_L^0 \rightarrow \pi^\pm e^\mp \nu_e$), respectively. Also the ratio (30) is derived from semileptonic B decays. Since all these decays practically don't involve the Higgs sector (the couplings of the Higgs to leptons are in general of the order of lepton masses, i.e., negligible), we can argue that the restrictions (29) and (30) apply not just to the MSM, but to a large class of standard models with extended Higgs sectors, including the present 2HDSM framework.

We performed the analysis of the K^0 - \bar{K}^0 and B_d^0 - \bar{B}_d^0 mixing according to the formulas presented above, taking into account the uncertainties in the experimental data for $\Delta M_{B_H^0-B_L^0}$ (24) and the hadronic uncertainties (26), (27) [or (28)]. The two relative uncertainties in $\Delta M_{B_H^0-B_L^0}$ and $F_B\sqrt{B_B}$ in (23) are regarded as independent and are combined by taking the square root of the sum of their squares. In order to account for the uncertainty in the CKM parameters ζ_j 's, we scanned the allowed CKM parameter region (29)-(30) in the $\sin \theta_{13}$ vs $\sin \theta_{23}$ plane with 169 points (13×13) that are uniformly distributed over that region in each direction. We allowed the CP-violating phase δ in the CKM matrix V to be free, and took for the top quark mass $m_t^{\text{phy}} = 175 \text{ GeV}$, as motivated by the CDF results [14]. The mass m_t taken in the loop-integrands (20) and (21) in parameters $x_3 (= m_t^2/M_W^2)$ and $y_3 (= m_t^2/M_{H^\pm}^2)$ was not the pole mass m_t^{phy} , but the running mass $m_t(m_t) \approx 167 \text{ GeV}$ (this point was discussed in Ref. [10]). Then, choosing a specific value for M_{H^\pm} , we obtain the allowed intervals of values of the normalized Yukawa coupling $|X^{(U)}(m_t)| = [|U_{33}(m_t)|v/(\sqrt{2}m_t(m_t))]$ for a chosen CKM angle δ . We depicted these allowed regions in the plane δ vs $|X^{(U)}(m_t)|$ in Figs. 3a, 3b, 3c, for the values of the charged Higgs mass $M_{H^\pm} = 200, 400, 600 \text{ GeV}$, respectively. The solid and dash-dotted lines (and the δ -axis) delimit the allowed region for the case of the more restricted bounds (28) on the hadronic matrix elements that are favored by the QCD sum rules and lattice calculations; the dashed and dash-dot-dotted lines (and the δ -axis) delimit the allowed region for the case of less restrictive bounds (26) and (27). The somewhat bumpy solid lines in these figures are a consequence of the fact that we scanned the allowed region of the CKM parameter plane $\sin \theta_{13}$ vs $\sin \theta_{23}$ with 169 points only; increasing the number of points further would lead to more continuous slopes of the border lines and would increase the solid and the dashed lines by at most a few percent, as our numerics suggests. From these figures we see the following behavior. The Yukawa coupling $|X^{(U)}(m_t)|$ has in the case of a lighter charged Higgs a more stringent upper bound; this upper bound remains always safely in the region $\mathcal{O}(1)$; however, it depends rather strongly on the chosen bounds for the hadronic matrix element parameters B_K and $F_B\sqrt{B_B}$ (26)-(28). Also the allowed region for the CP-violating CKM angle δ depends rather strongly on these allowed values. It is the B_d^0 - \bar{B}_d^0 mixing that restricts the angle δ from above. Furthermore, the larger the Yukawa coupling $|X^{(U)}|$ is, the smaller is the allowed interval for δ . If m_t^{phy} is increased, the upper bound on $|X^{(U)}|$ decreases somewhat. In the special 2HDSM(II) and (I), the vertical axis $|X^{(U)}(m_t)|$ is to be replaced by $\cot \beta$, according to (10) and (11). In this case, Figs. 3 would give us lower bounds for $\tan \beta$. Furthermore, once the experimental and theoretical uncertainties are reduced sufficiently, the lower bounds on $|X^{(U)}(m_t)|$ (the dash-dotted lines in Figs. 3a-c) may increase in such a way that they don't cut the x-axis (the line $|X^{(U)}(m_t)| = 0$), i.e., the MSM would become ruled out in such a case and we would

⁹ In the *Review of Particle Properties* [11] this angle is denoted as δ_{13} .

obtain a nonzero lower bound on $|X^{(U)}(m_t)|$.

4.) D - \bar{D} mixing in a general 2HDSM framework

For the phenomenon of the D^0 - \bar{D}^0 mixing, the short distance contribution at one loop is also represented by the diagrams of Fig. 1. However, now the external quark legs are of the up-type ($c\bar{u}$, $\bar{c}u$), and therefore the inner quark propagators are of the down-type. In the MSM, it turns out that the effect of the mass of external c -quark, when combined with the GIM mechanism, influences crucially the strength of the resulting four-fermion couplings [15]. A relation analogous to the B_d^0 - \bar{B}_d^0 relation (23) results in the MSM prediction for the short distance contribution to ΔM_{D^0} ($= |m_{D^0} - m_{\bar{D}^0}|$): $\Delta M_{D^0} \simeq 5 \cdot 10^{-18} GeV$ (when taking $F_D \simeq 0.2 GeV$ and $B_D \simeq 1$) [16]. However, long distance contributions, e.g. $\pi\pi$ and KK intermediate states, give somewhat higher contributions to ΔM_{D^0} : the intermediate particle dispersive approach [17] gives $\Delta M_{D^0} \simeq 10^{-16} GeV$, and the heavy quark effective theory approach [18] gives $\Delta M_{D^0} \simeq 10^{-17} GeV$. On the other hand, the present experimental upper bound for ΔM_{D^0} ($\Delta M_{D^0} < 1.3 \cdot 10^{-13} GeV$) is still crude [11] and far above these values. Experiments with large expected numbers ($\sim 10^8$) of reconstructed charm mesons are being planned. These could probe whether the present upper bound should be decreased by a factor $10^{-1} - 10^{-2}$, i.e., whether $\Delta M_{D^0} \lesssim 10^{-15} GeV$ or not. This would make the D -physics more interesting, giving us possible experimental evidence for physics beyond the MSM.

Within the present framework, the HH box diagram of Fig. 1 with two b -quark propagators is the dominant contribution to ΔM_{D^0} , as long as the Yukawa coupling D_{33} ($\rightarrow X^{(D)}$) is large enough for \mathcal{A}_{HH}^D [$\propto (D_{33})^4$] to dominate over both the MSM short distance amplitude \mathcal{A}_{WW}^D and over the mixed amplitude \mathcal{A}_{HW}^D [$\propto (D_{33})^2$]. Therefore, we will demand that the contribution of \mathcal{A}_{HH}^D to ΔM_{D^0} not exceed the present experimental upper bound $1.3 \cdot 10^{-13} GeV$. Since the GIM mechanism, which suppresses the MSM contributions, is not relevant for such diagrams, and $m_b > m_c$, it is justifiable to ignore the effects of the mass of the external c quark. Calculation analogous to that of the K^0 - \bar{K}^0 and B_d^0 - \bar{B}_d^0 mixing, but with the QCD corrections ignored, yields for $D^0 \rightarrow \bar{D}^0$

$$\mathcal{L}_{eff}^{HH} = \mathcal{A}_{HH}^D \left[\overline{u(x)^a} \gamma^\mu \left(\frac{1 - \gamma_5}{2} \right) c(x)^a \right]^2, \quad (31)$$

$$\mathcal{A}_{HH}^D = -\frac{1}{128\pi^2 M_{H^\pm}^2} (\zeta_b)^2 [D_{33}(m_b)]^4 \mathcal{I}(y_b, y_b). \quad (32)$$

Here, we denoted $\zeta_b = V_{cb}^* V_{ub}$ and $y_b = (m_b/M_{H^\pm})^2$. The integral for \mathcal{I} is written in (17), and has the value $\mathcal{I}(y_b, y_b) = 1 + \mathcal{O}(y_b \ln y_b)$. Denoting by F_D and B_D the hadronic matrix element parameters, analogously as in the case of the B_d^0 - \bar{B}_d^0 mixing (27), we get the condition

$$\left(\Delta M_D^{HH} = \right) \left| \mathcal{A}_{HH}^D \right| \frac{2}{3} F_D^2 B_D M_D < 1.3 \cdot 10^{-13} GeV, \quad (33)$$

which in turn gives us the upper bound on the Yukawa coupling $D_{33}(m_b)$ [$\rightarrow X^{(D)}(m_b)$, cf. (9)]

$$|X^{(D)}(m_b)| \left(= \frac{|D_{33}(m_b)|v}{\sqrt{2}m_b(m_b)} \right) \lesssim 26 \sqrt{\frac{M_{H^\pm}}{GeV}} (1 \pm 0.28). \quad (34)$$

In this upper bound, (± 0.28) denotes the uncertainty arising from the experimental uncertainty in the CKM parameter ζ_b (47 percent) and from the theoretical uncertainty in F_D [we took: $F_D = 0.2 GeV(1 \pm 0.3)$, $B_D \simeq 1$]. Taking on the right-hand side of (34) the central value, we obtain for the case of $M_{H^\pm} = 200 GeV$ the upper bound $|X^{(D)}(m_b)|^{UB} \approx 362$,

which is by factor 3 above the perturbative limit (12). On the other hand, if assuming that future experiments decreased the upper bound $(\Delta M_{D^0})^{UB}$ by two orders of magnitude [to $\mathcal{O}(10^{-15} GeV)$], the present framework would give as a result $|X^{(D)}(m_b)| \lesssim 8\sqrt{M_{H^\pm}/GeV}$. For the case of $M_{H^\pm} = 200 GeV$ this would imply $|X^{(D)}(m_b)| \lesssim 110$, which is roughly at the perturbative limit (12).

In order to estimate the most stringent possible constraints imposed on $X^{(D)}$ by any future measurements of ΔM_{D^0} , we argue in the following way. If we assume that at some future time the value of ΔM_{D^0} is well measured and turns out to be sufficiently above the value estimated by the MSM, then the discussed general 2HDSM framework will still remain a viable framework, in which the HW and HH exchange diagrams of Fig. 1 (with b -quark propagators) are responsible for the deviation from the MSM prediction. The HH diagrams would then give a contribution $(\Delta M_{D^0})^{HH}$ of an order of magnitude at least as large as the order of magnitude of the estimated MSM contributions ($10^{-17} GeV$). Here we assume that the computed latter contributions (the long distance contributions) will remain uncertain by a factor of $\mathcal{O}(1)$, say a factor 2-3. This would imply that the 2HDSM's can be successfully distinguished from the MSM by the measurement of $|\Delta M_{D^0}|$ only if

$$|(\Delta M_{D^0})^{HH}| \gtrsim 10^{-17} GeV \implies |X^{(D)}(m_b)| \gtrsim 2.4\sqrt{M_{H^\pm}/GeV}.$$

This is then approximately the lowest possible value of $|X^{(D)}(m_b)|$ that can be inferred from any future measurements of $|\Delta M_{D^0}|$. Here, we took the central value $1.4 \cdot 10^{-4}$ for ζ_b , and $F_D = 0.2 GeV$. Assuming $M_{H^\pm} \gtrsim 200 GeV$, this would give $|X^{(D)}(m_b)|^{\text{lowest}} \simeq 34$, well below the perturbative limit [Eq. (12)]. In the special case of the 2HDSM(II), this would imply $|X^{(U)}|^{\text{highest}} (= \cot \beta) \approx 0.03$. This means that within the 2HDSM(II) any future measurements of ΔM_{D^0} would provide us with an estimated value for $\cot \beta$ only if $\cot \beta < 0.03$ ($\tan \beta > 35$). If $\tan \beta < 35$, these measurements would not be able to distinguish between the MSM and 2HDSM(II), and would only give an upper bound $(\tan \beta)^{UB} \simeq 35$ that would result in HH contributions comparable to the theoretical uncertainties of the MSM long distance contributions to ΔM_{D^0} .

From these considerations we conclude that the future (low energy) measurements of ΔM_{D^0} will become important for identifying a possible 2HDSM physics beyond the MSM and for estimating the Yukawa parameter $|X^{(D)}(m_b)|$ only in the case that the actual value of the latter parameter is large enough: $|X^{(D)}(m_b)| \gtrsim 2.4 \cdot \sqrt{M_{H^\pm}/GeV}$ (for 2HDSM(II): if $\tan \beta \gtrsim 2.4\sqrt{M_{H^\pm}/GeV}$), provided that the theoretical prediction of the long distance MSM contributions remains uncertain by a factor $\mathcal{O}(1)$. If $|X^{(D)}(m_b)|$ is smaller than this value, the measurements of ΔM_{D^0} would not be able to distinguish between the 2HDSM's and the MSM, and would only provide us with the upper bound $|X^{(D)}(m_b)|^{UB} \simeq 2.4\sqrt{M_{H^\pm}/GeV}$.

At this point, we are able to estimate the upper bound on some of the (small) off-diagonal FCNC elements of the renormalized Yukawa matrices $U^{(j)}$ and $D^{(j)}$ ($j = 1, 2$) of the starting Lagrangian (3) (in the mass basis). As stated in the Introduction, in the present framework we assume that these FCN Yukawa couplings are sufficiently suppressed, so that the calculated one-loop box-diagrams (cf. Fig. 1) with charged Higgs give contributions to the considered meson-antimeson mixings which dominate over the direct tree level contributions. It was this requirement that allowed us to ignore the off-diagonal elements in $U^{(j)}$ and $D^{(j)}$ and to set them formally equal to zero. The tree level contributions of such (small) FCN Yukawa couplings to the meson-antimeson mixings represent an exchange of a neutral Higgs H^0 between the corresponding initial $q_k \bar{q}_\ell$ and the final $\bar{q}_k q_\ell$ state ($k \neq \ell$). It is straightforward to check that the resulting electroweak amplitudes in front of the effective

four-fermion terms in the case of the $K^0\text{-}\bar{K}^0$ mixing are $\mathcal{A}_{\text{tree}}^K \sim (D_{12}^{(j)})^2/(2M_{H^0}^2)$ ($j = 1, 2$) and that they are *real* (if the phase between the VEV's is $\xi = 0$). Also, the corresponding hadronic matrix elements of the four-fermion terms are real. Therefore, these amplitudes cannot affect the presented analysis of the $K^0\text{-}\bar{K}^0$ mixing, because the relevant quantity there was $\text{Im}(\mathcal{A}^K)$. These tree amplitudes are of the order of $(D_{ab}^{(j)})^2/(2M_{H^0}^2)$ and $(U_{cd}^{(j)})^2/(2M_{H^0}^2)$ for the $B_d^0\text{-}\bar{B}_d^0$ and $D^0\text{-}\bar{D}^0$ mixing, respectively, where the indices are: $(ab) = (13), (31)$ and $(cd) = (12), (21)$, and $j = 1, 2$. On the other hand, the corresponding box diagrams (cf. Fig. 1) resulted in the amplitudes $\mathcal{A}_{HH}^B \sim (\zeta_t^B)^2 \mathcal{I}(y_t, y_t) |U_{33}|^4 / (128\pi^2 M_{H^\pm}^2) \sim 10^{-3} (\zeta_t^B)^2 |U_{33}|^4 / M_{H^-}^2$, and $\mathcal{A}_{HH}^D \sim 10^{-3} (\zeta_b^D)^2 |D_{33}|^4 / M_{H^-}^2$. Assuming that $M_{H^0} \sim M_{H^\pm}$, and taking $U_{33} \sim U_{33}^{(k)}$, $D_{33} \sim D_{33}^{(k)}$ [cf. Eq. (6)], we then arrive at the following upper bounds for off-diagonal elements of the Yukawa matrices $U^{(j)}$ and $D^{(j)}$:

$$\frac{|D_{13}^{(j)}|}{|U_{33}^{(k)}|^2}, \frac{|D_{31}^{(j)}|}{|U_{33}^{(k)}|^2} \lesssim \mathcal{O}(10^{-3}), \quad \frac{|U_{12}^{(j)}|}{|D_{33}^{(k)}|^2}, \frac{|U_{21}^{(j)}|}{|D_{33}^{(k)}|^2} \lesssim \mathcal{O}(10^{-5}), \quad (j, k = 1, 2). \quad (35)$$

Since the requirement of perturbativity of the theory (12) says that $|U_{33}|, |D_{33}| \leq \mathcal{O}(1)$, and since in general $U_{33} \sim U_{33}^{(k)}$ and $D_{33} \sim D_{33}^{(k)}$, we get the bounds $|D_{13}^{(j)}|, |D_{31}^{(j)}| \lesssim \mathcal{O}(10^{-3})$ and $|U_{12}^{(j)}|, |U_{21}^{(j)}| \lesssim \mathcal{O}(10^{-5})$ ($j, k = 1, 2$). These two constraints are the conditions for the presented analysis of the $B\text{-}\bar{B}$ and $D\text{-}\bar{D}$ mixing, respectively, to hold. Furthermore, the analysis of the $b \rightarrow s\gamma$ decay (in Section 5) does not require any additional restrictions on the FCN Yukawa couplings, because this decay cannot occur at the tree level.

5.) The decay $b \rightarrow s\gamma$ in a general 2HDSM framework

Among the loop-induced FCNC's, the $b \rightarrow s\gamma$ decay is especially important because its strength may strongly depend on a possible new physics, and because it has a relatively strong rate - most of the other FCNC processes involving photons or leptons are suppressed relatively to $b \rightarrow s\gamma$ by an order of α_{em} . The long range QCD interactions are here not important because $m_b \gg \Lambda_{QCD}$. Therefore, the following approximation is usually used (spectator model):

$$\frac{\Gamma(B \rightarrow X_s \gamma)}{\Gamma(B \rightarrow X_c e \bar{\nu}_e)} \approx \frac{\Gamma(b \rightarrow s \gamma)}{\Gamma(b \rightarrow ce \bar{\nu}_e)}. \quad (36)$$

The normalization to the semilpetonic rate $\Gamma(b \rightarrow ce \bar{\nu}_e)$ eliminates uncertainties of the CKM matrix element V_{ts} and of the factor m_b^5 in the decay width $\Gamma(b \rightarrow s\gamma)$. The recent CLEO report [19] gives the measured branching ratio

$$B(b \rightarrow s\gamma) = \frac{\Gamma(b \rightarrow s\gamma)}{\Gamma(b \rightarrow \text{all})} = (2.32 \pm 0.67) \cdot 10^{-4}. \quad (37)$$

This implies, at 90 percent confidence level (CL)

$$B(b \rightarrow s\gamma) = (2.3 \pm 1.1) \cdot 10^{-4}. \quad (38)$$

The predicted range for the MSM ($2.0 \cdot 10^{-4} < B(b \rightarrow s\gamma) < 3.8 \cdot 10^{-4}$) [20]-[21] is still fairly compatible with the above measurement.

The short distance QCD effects in this decay are drastic and enhance the rate by several factors [20]-[23]. This decay is the only known process dominated by the two-loop contributions (i.e., leading QCD corrections). Here we use the formula for the branching ratio derived by the method of operator product expansion as given in Ref. [23] and based on the work of [22]

$$B(b \rightarrow s\gamma) = \frac{|V_{ts}^* V_{tb}|^2}{|V_{cb}|^2} \frac{6\alpha_{em}}{\pi g(z)} |C_7^{(0)eff}(\mu)|^2, \quad (39)$$

where

$$C_7^{(0)eff}(\mu) = \eta^{16/23} C_7^{(0)}(M_W) + \frac{8}{3} \left(\eta^{14/23} - \eta^{16/23} \right) C_8^{(0)}(M_W) + C_2^{(0)}(M_W) \sum_{j=1}^8 h_j \eta^{a_j} . \quad (40)$$

We denoted $z = m_c^{\text{phy}}/m_b^{\text{phy}}$ ($\simeq 0.32$), $\eta = \alpha_s(M_W^2)/\alpha(\mu^2)$, and

$$g(z) = 1 - 8z^2 + 8z^6 - z^8 - 24z^4 \ln z . \quad (41)$$

The function $g(z)$ is the phase space factor for the semileptonic decay $b \rightarrow ce\bar{\nu}_e$. The numbers h_j and a_j are given in Ref. [23] and are based on Ref. [22]. We mention that the sum of h_j 's is zero. $C_j^{(0)}(M_W)$ are Wilson coefficients at some high scale [taken to be M_W ($\sim m_t \sim M_{H^\pm}$)] where the QCD corrections are assumed to be negligible¹⁰

$$C_2^{(0)}(M_W) = 1 , \quad C_j^{(0)}(M_W) = C_j^{(0)W}(M_W) + C_j^{(0)H}(M_W) , \quad (j = 7, 8) , \quad (42)$$

$$\begin{aligned} C_7^{(0)W}(M_W) &= \frac{3x^3 - 2x^2}{4(x-1)^4} \ln x + \frac{-8x^3 - 5x^2 + 7x}{24(x-1)^3} , \\ C_8^{(0)W}(M_W) &= \frac{-3x^2}{4(x-1)^4} \ln x + \frac{-x^3 + 5x^2 + 2x}{8(x-1)^3} , \end{aligned} \quad (43)$$

$$\begin{aligned} C_7^{(0)H}(M_W) &= X^{(U)} X^{(D)} \left[\frac{3y^2 - 2y}{6(y-1)^3} \ln y + \frac{-5y^2 + 3y}{12(y-1)^2} \right] + \\ &\quad + \left(X^{(U)} \right)^2 \left[\frac{3y^3 - 2y^2}{12(y-1)^4} \ln y + \frac{-8y^3 - 5y^2 + 7y}{72(y-1)^3} \right] , \\ C_8^{(0)H}(M_W) &= X^{(U)} X^{(D)} \left[\frac{-y}{2(y-1)^3} \ln y + \frac{-y^2 + 3y}{4(y-1)^2} \right] + \\ &\quad + \left(X^{(U)} \right)^2 \left[\frac{-y^2}{4(y-1)^4} \ln y + \frac{-y^3 + 5y^2 + 2y}{24(y-1)^3} \right] . \end{aligned} \quad (44)$$

We denoted $x = (m_t/M_W)^2$ and $y = (m_t/M_{H^\pm})^2$. $C_7^{(0)W}$ and $C_7^{(0)H}$ are Wilson coefficients associated with the leading one-loop electroweak diagrams generating the $b \rightarrow s\gamma$ transition (Figs. 4a, b, respectively), i.e., these diagrams induce the term

$$\mathcal{L}_{eff}^{ew} = \frac{G_F}{\sqrt{2}} V_{ts}^* V_{tb} C_7^{(0)}(M_W) \hat{\mathcal{O}}_7 , \quad \hat{\mathcal{O}}_7 = \frac{e_0}{8\pi^2} m_b \bar{s}_a \sigma^{\mu\nu} (1 + \gamma_5) b^a F_{\mu\nu} , \quad (45)$$

where $\sigma^{\mu\nu} = \frac{i}{2} [\gamma^\mu, \gamma^\nu]$ and $F_{\mu\nu}$ is the usual QED field strength tensor. Note that $C_7^{(0)eff}(\mu = M_W) = C_7^{(0)}(M_W)$, i.e., this is the contribution when we ignore the QCD effects. Similarly, $C_8^{(0)W}(M_W)$ and $C_8^{(0)H}(M_W)$ are Wilson coefficients corresponding to an analogous operator, but with $F_{\mu\nu}$ replaced by the corresponding gluon field strength tensor $G_{\mu\nu}^a$, i.e., they can be derived from the one-loop diagrams of Figs. 4a,b, respectively, when we replace the photon external leg by a gluon external leg. One new element in Eqs. (43)-(44) are the expressions for $C_j^{(0)H}$ ($j=7,8$), corresponding to the diagrams of Fig. 4b. These expressions have been written in the literature for the special cases of the 2HDSM(I) and (II); here, they are

¹⁰ This scale M_W may be somewhat too low, especially if M_{H^\pm} is high: $M_{H^\pm} > 200\text{GeV}$.

valid for the discussed general 2HDSM framework. As we see, they involve *both* normalized Yukawa couplings of the charged Higgs: $X^{(U)}(E)$ and $X^{(D)}(E)$. Therefore, this fact will provide us with interesting constraints on the framework in the plane $X^{(U)}$ vs $X^{(D)}$. As already argued in Section 3, the effective energy of probes E in the couplings $X^{(U)}(E)$ and $X^{(D)}(E)$ in Eq. (44) is $E \approx m_t$, because the top quark gives the dominant contributions to the relevant 1-loop diagrams (cf. Fig. 4b).

In the calculation, we take the low energy cut-off μ to be $\mu = m_b \simeq 4.9 \text{ GeV}$; $\alpha_s(M_W^2) \simeq 0.119$, $\alpha_s(m_b^2) \simeq 0.22$, $|V_{ts}^* V_{tb}|^2 / |V_{cb}|^2 \simeq 0.95$; $m_c^{\text{phy}} / m_b^{\text{phy}} \simeq 0.32$; $\alpha_{em}(m_b^2) \simeq \alpha_{em}(1 \text{ GeV}^2) \simeq 1/137$, $B(b \rightarrow ce\bar{\mu}_e) \approx B(b \rightarrow e\bar{\mu}_e + \text{anything}) \simeq 0.104$. By the same argument as in the case of the B - \bar{B} and K - \bar{K} mixing, we take for $m_t(E)$ in the parameters x and y in Eqs. (43) and (44) the value $m_t(m_t) \simeq 167 \text{ GeV}$, which corresponds to $m_t^{\text{phy}} = 175 \text{ GeV}$. With these input data, the MSM prediction [i.e., when setting $C_j^{(0)H}(M_W) = 0$ in (42) and (40)] is: $B(b \rightarrow s\gamma)^{\text{MSM}} \simeq 2.90 \cdot 10^{-4}$. As discussed in Ref. [23], the major uncertainties in the formula (39)-(40) come from the μ -dependence of the QCD parameter $\eta = \alpha_s(M_W^2) / \alpha_s(\mu^2)$ ($m_b/2 < \mu < 2m_b$). This theoretical uncertainty, together with other experimental and theoretical uncertainties, would result in an uncertainty of up to 30 percent in this formula [23]. Combining this 30 percent uncertainty with the 90 percent CL result (38) of CLEO, we obtain the following limits for the allowed values of the formula (39):

$$0.92 \cdot 10^{-4} < B(b \rightarrow s\gamma)^{\text{th.}} < 4.86 \cdot 10^{-4}.$$

The superscript “th.” denotes the expression (39)-(40). For chosen values $M_{H^\pm} = 200, 400, 600 \text{ GeV}$, these limits in the discussed 2HDSM framework result in the allowed regions of the plane $X^{(U)}(m_t)$ vs $X^{(D)}(m_t)$ as depicted in Figs. 5a,b,c, respectively. For comparison, the dashed line in these figures represents the region of the 2HDSM(II) ($X^{(D)} = 1/X^{(U)} = \tan \beta$), and the dash-dotted line the region of the 2HDSM(I) ($X^{(D)} = -X^{(U)} = -\cot \beta$). Incidentally, we see from Fig. 5a that in the case of $M_{H^\pm} = 200 \text{ GeV}$ the line for the 2HDSM(II) lies entirely outside the allowed region, i.e., in the “type II” model we must have $M_{H^\pm} > 200 \text{ GeV}$ as a consequence of the $b \rightarrow s\gamma$ data. In Figs. 5a-c we included only those regions for $X^{(U)}$ which were allowed by B_d^0 - \bar{B}_d^0 and $K^0 - \bar{K}^0$ mixing for the choice (28) of the range of the hadronic parameters B_K and $F_B \sqrt{B_B}$ (cf. Figs. 3a-c).

6.) Conclusions

From the presented discussion we infer that the future improved experimental data for the B - \bar{B} , K - \bar{K} and D - \bar{D} mixing and for the $b \rightarrow s\gamma$ decay, as well as the future reduced theoretical uncertainties for the hadronic matrix elements, can further severely constrain the (dominant) Yukawa couplings $X^{(U)}$, $X^{(D)}$ of the charged Higgs. If the experimental data are improved sufficiently and the theoretical hadronic uncertainties reduced sufficiently, then the analyses such as the one presented here may in a foreseeable future be able to rule out the minimal SM and even certain special types of the 2HDSM’s (e.g., the popular “type II”, and “type I” 2HDSM). In such a case, a more general 2HDSM framework discussed here could still survive as a viable framework. We note that this can be achieved by analysing *low* energy physics alone - the meson-antimeson mixings and the b decays are phenomena at low energy. If the charged Higgs is found in high energy experiments and its mass measured, this mass will represent important new information. This information would greatly facilitate the analyses of low energy phenomena and would help to either rule out or to favor various specific 2HDSM scenarios that are contained in the discussed 2HDSM framework.

Acknowledgments

The author would like to thank to E.A. Paschos for bringing to his attention the question of general 2HDSM frameworks with suppressed FCNC's, and to P. Overmann and A. Datta for helpful and stimulating discussions.

References

- [1] E.A. Paschos, Phys. Rev. **D15** (1977) 1966; S.L. Glashow and S. Weinberg, Phys. Rev. **D15** (1977) 1958
- [2] R. Gatto, G. Morchio, G. Sartori, F. Strocchi, Nucl. Phys. B163, 221 (1980); K. Kang and A.C. Rothman, Phys. Rev. D22, 2869 (1980)
- [3] Y.-L. Wu, Carnegie-Mellon preprint CMU-HEP-94-17 (hep-ph/9406306); Y.-L. Wu and L. Wolfenstein, Phys. Rev. Lett. 73, 1762 (1994);
- [4] T.P. Cheng and M. Sher, Phys. Rev. D35, 3484 (1987); L.J. Hall and S. Weinberg, Phys. Rev. D48, 979 (1993)
- [5] V. Barger, J.L. Hewett and R.J.N. Phillips, Phys. Rev. D41, 3421 (1990); J.F. Gunion and B. Grzadkowski, Phys. Lett. **B243** (1990) 301; A.J. Buras, P. Krawczyk, M.E. Lautenbacher and C. Salazar, Nucl. Phys. **B337** (1990) 284
- [6] T. Inami and C.S. Lim, Prog. Theor. Phys. 65, 297 (1981), (E) 1772
- [7] A.I. Vainshtein, V.I. Zakharov and M.A. Shifman, JETP 45, 670 (1977); V. Vysotskii, Sov. J. Nucl. Phys. 31, 797 (1980)
- [8] A. Datta, J. Fröhlich and E.A. Paschos, Z. Phys. C46, 63 (1990)
- [9] F.J. Gilman and M.B. Wise, Phys. Rev. D20, 2392 (1979), Phys. Rev. D27, 1128 (1983)
- [10] A.J. Buras, M. Jamin and P.H. Weisz, Nucl. Phys. B347, 491 (1990)
- [11] Particle Data Group, *Review of Particle Properties*, Phys. Rev. D45 (June 1992) and Phys. Rev. D50 (August 1994)
- [12] CLEO Collaboration, F. Bartelt *et al.*, Phys. Rev. Lett. 71, 4111 (1993)
- [13] ARGUS Collaboration, H Albrecht *et al.*, Phys. Lett. B255, 297 (1991)
- [14] CDF Collaboration, F. Abe *et al.*, Phys. Rev. D50, 2966 (1994)
- [15] A. Datta, D. Kumbhakar, Z. Phys. C27, 515 (1985); H.-Y. Cheng, Phys. Rev. D26, 143 (1982); A.J. Buras, W. Słominski and H. Steger, Nucl. Phys. B245, 369 (1984)
- [16] J.L. Hewett, SLAC preprint SLAC-PUB-6674 (1994), hep-ph/9409379
- [17] J. Donoghue, E. Golowich, B.R. Holstein and J. Trampetić, Phys. Rev. D33, 179 (1986)
- [18] H. Georgi, Phys. Lett. B297, 353 (1992); T. Ohl, G. Ricciardi and E.H. Simmons, Nucl. Phys. B403, 605 (1993)
- [19] J. Ernst, Rochester preprint UR 1381-94, to appear in *Proceedings of the Eighth Meeting of the Division of Particles and Fields*, Albuquerque, 1994

- [20] S. Bertolini, F. Borzumati and A. Masiero, Phys. Rev. Lett. 59, 180 (1987); N.G. Deshpande, P. Lo, J. Trampetić, G. Eilam and P. Singer, *ibid* 59, 183 (1987); R. Grigjanis, P.J. O'Donnell and M. Sutherland, Phys. Lett. B224, 209 (1989); G. Cella, G. Curci, G. Ricciardi and A. Vicere, Phys. Lett. B248, 181 (1990)
- [21] B. Grinstein, R. Springer and M.B. Wise, Phys. Lett. B202, 138 (1988)
- [22] M. Ciuchini, E. Franco, G. Martinelli, L. Reina and L. Silvestrini, Phys. Lett. B316, 127 (1993); M. Ciuchini, E. Franco, L. Reina and L. Silvestrini, Phys. Lett. B334, 137 (1994)
- [23] A.J. Buras, M. Misiak, M. Münz and S. Pokorski, Nucl. Phys. B424, 374 (1994)

Figure Captions

Fig. 1: Box diagrams giving short distance contributions to meson-antimeson mixing ($P^0 = B^0, K^0, D^0$); solid lines denote quarks.

Figs. 2a-d: Various possible leading-log QCD corrections to the box diagrams; dash-dotted line denotes a gluon propagator.

Figs. 3a, 3b, 3c: The allowed regions in the plane δ vs $|X^{(U)}|$, for the values of the charged Higgs mass $M_{H^\pm} = 200, 400, 600 \text{ GeV}$, respectively. The solid and dash-dotted lines (and the δ -axis) delimit the allowed region for the case of the more restricted bounds (28) on the hadronic matrix elements; the dashed and dash-dot-dotted lines (and the δ -axis) delimit the allowed region for the case of less restrictive bounds (26) and (27).

Figs. 4a-b: The dominant one-loop contributions to the $b \rightarrow s\gamma$ decay. Besides the top quark propagator, the loops contain physical W^\pm (Fig. 4a) and physical H^\pm (Fig. 4b).

Figs. 5a-c: The regions in the $X^{(U)}(m_t)$ vs $X^{(D)}(m_t)$ plane that are allowed by the data on the $b \rightarrow s\gamma$ decay, for $M_{H^\pm} = 200, 400, 600 \text{ GeV}$, respectively. The allowed region is the central region between the four solid curves near the axes, and two separate stripes between the solid lines in the upper left and the lower right part of each graph. The dashed line corresponds to the special “type II” 2HDSM ($X^{(D)}(m_t) = 1/X^{(U)}(m_t) = \tan \beta$), and the dash-dotted line to the “type I” 2HDSM ($X^{(D)}(m_t) = -X^{(U)}(m_t) = -\cot \beta$).

This figure "fig1-1.png" is available in "png" format from:

<http://arxiv.org/ps/hep-ph/9411436v1>

This figure "fig2-1.png" is available in "png" format from:

<http://arxiv.org/ps/hep-ph/9411436v1>

This figure "fig1-2.png" is available in "png" format from:

<http://arxiv.org/ps/hep-ph/9411436v1>

This figure "fig1-3.png" is available in "png" format from:

<http://arxiv.org/ps/hep-ph/9411436v1>

This figure "fig1-4.png" is available in "png" format from:

<http://arxiv.org/ps/hep-ph/9411436v1>

This figure "fig1-5.png" is available in "png" format from:

<http://arxiv.org/ps/hep-ph/9411436v1>

This figure "fig1-6.png" is available in "png" format from:

<http://arxiv.org/ps/hep-ph/9411436v1>

Fig. 5a: $(b \rightarrow s \gamma)$; $M_{H^\pm} = 200 \text{ GeV}$

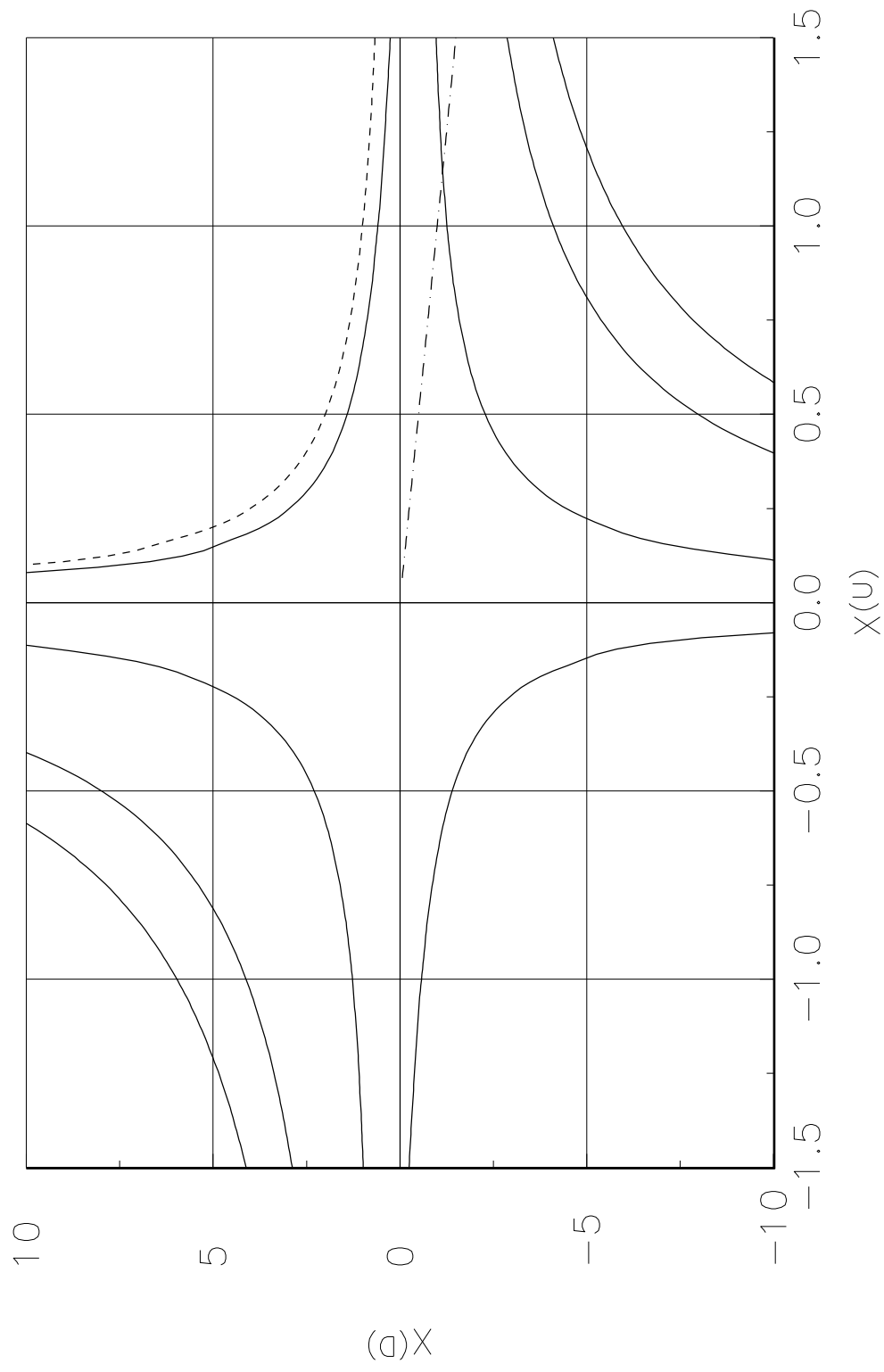


Fig. 3a: $M_{H^-} = 200$ GeV

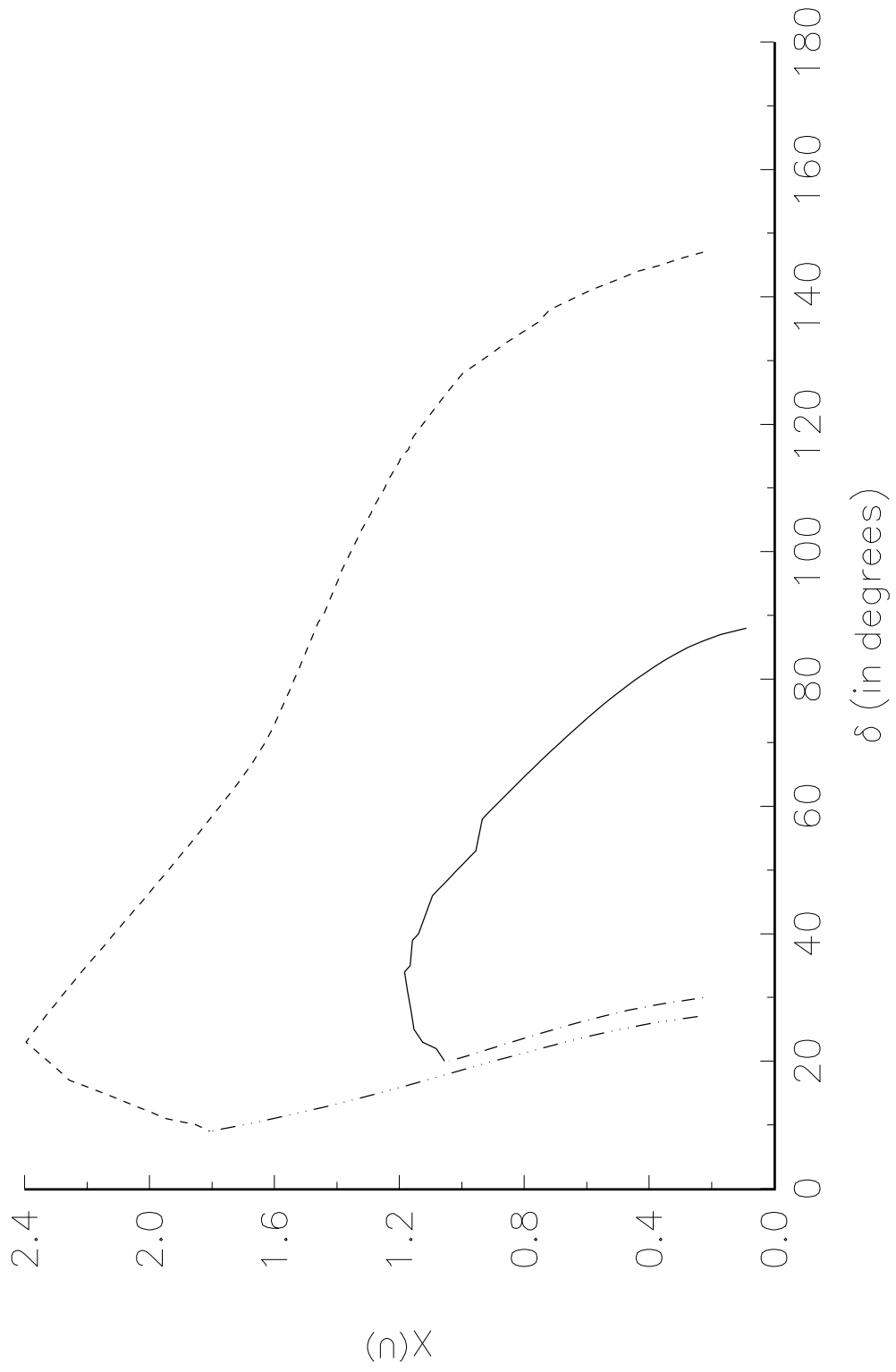


Fig. 5b: $(b \rightarrow s \gamma)$; $M_{H^\pm} = 400 \text{ GeV}$

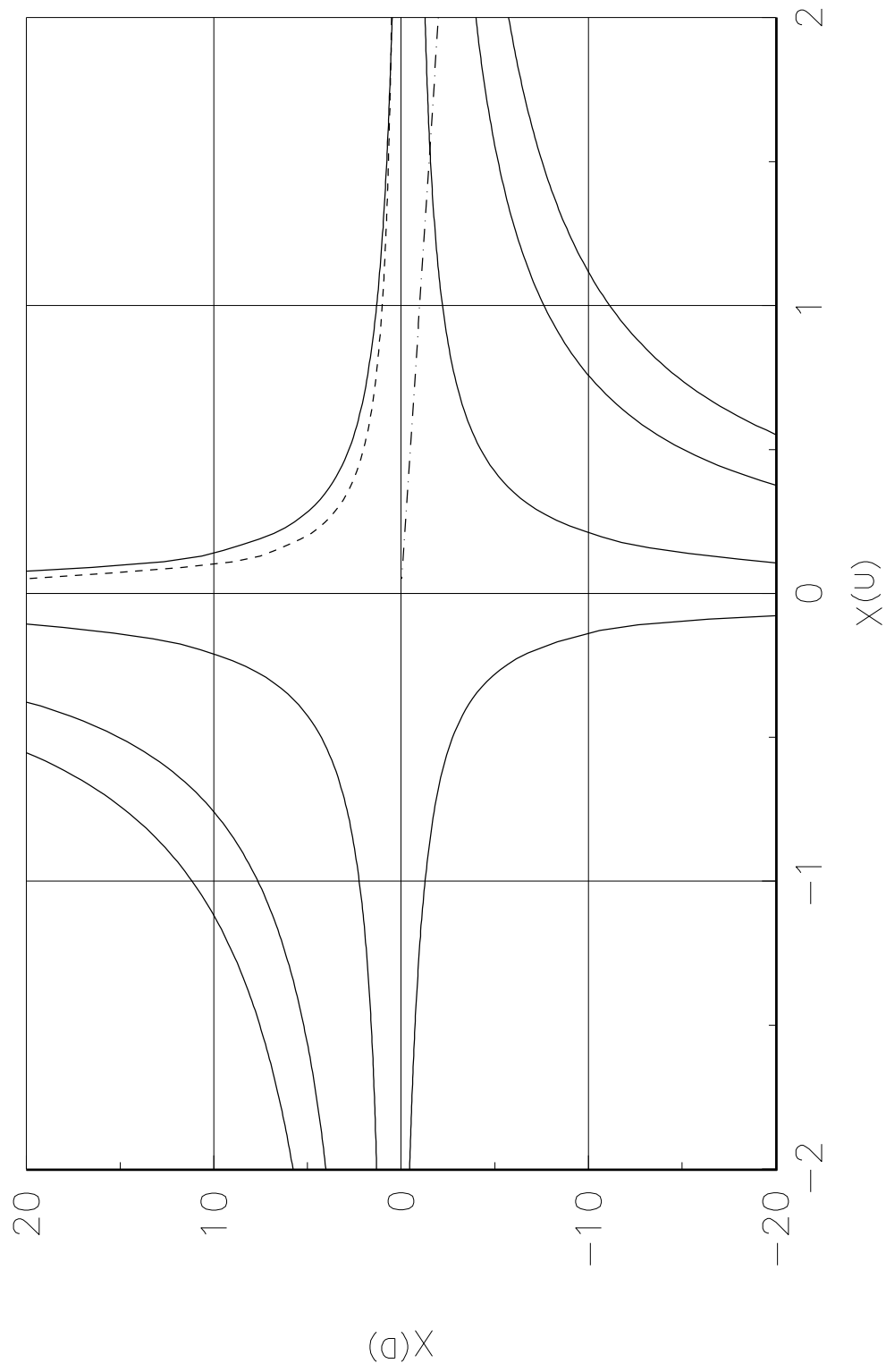


Fig. 3b: $M_{H^-} = 400$ GeV

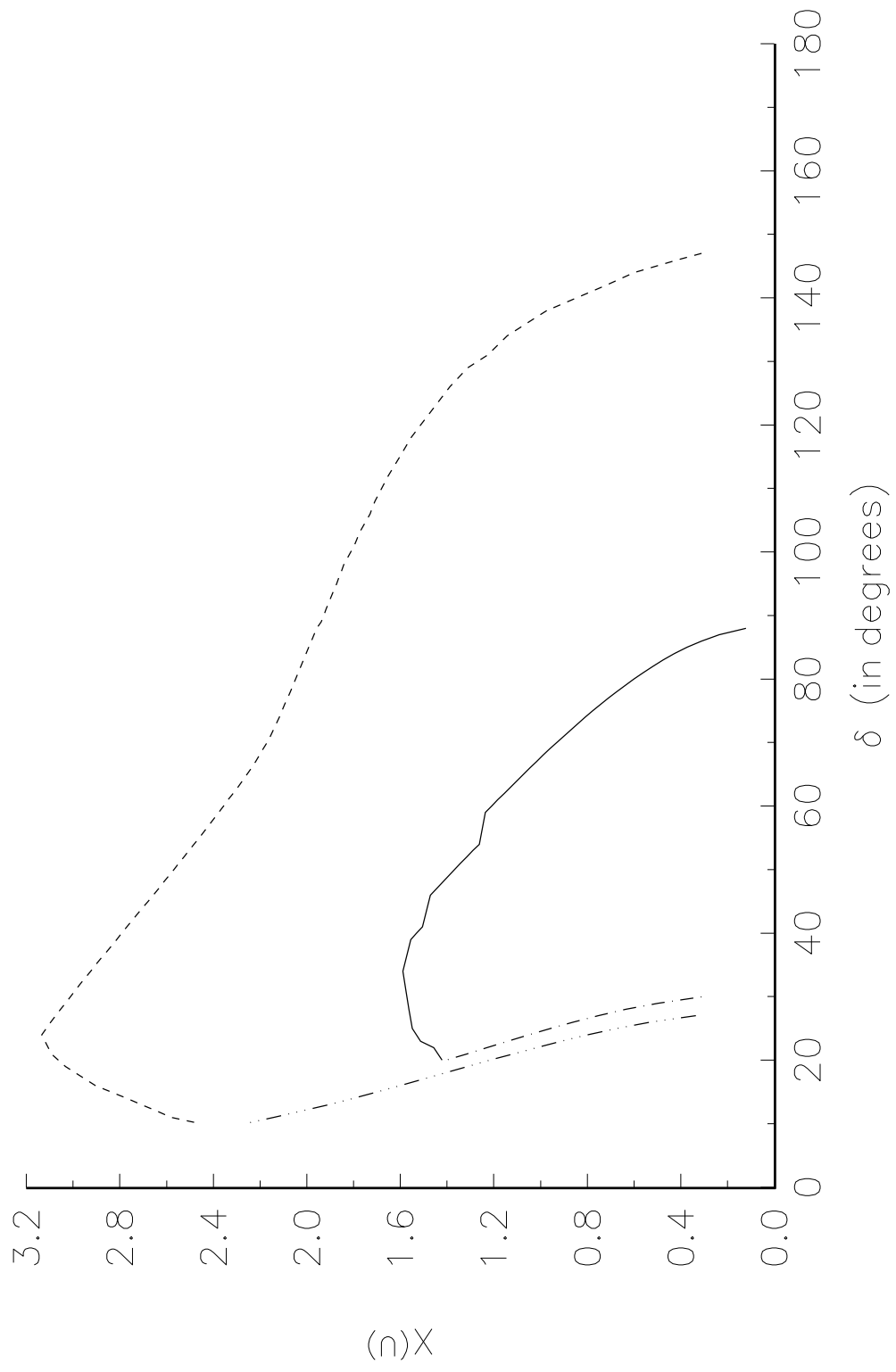


Fig. 5c: $(b \rightarrow s \gamma)$; $M_{H^\pm} = 600 \text{ GeV}$

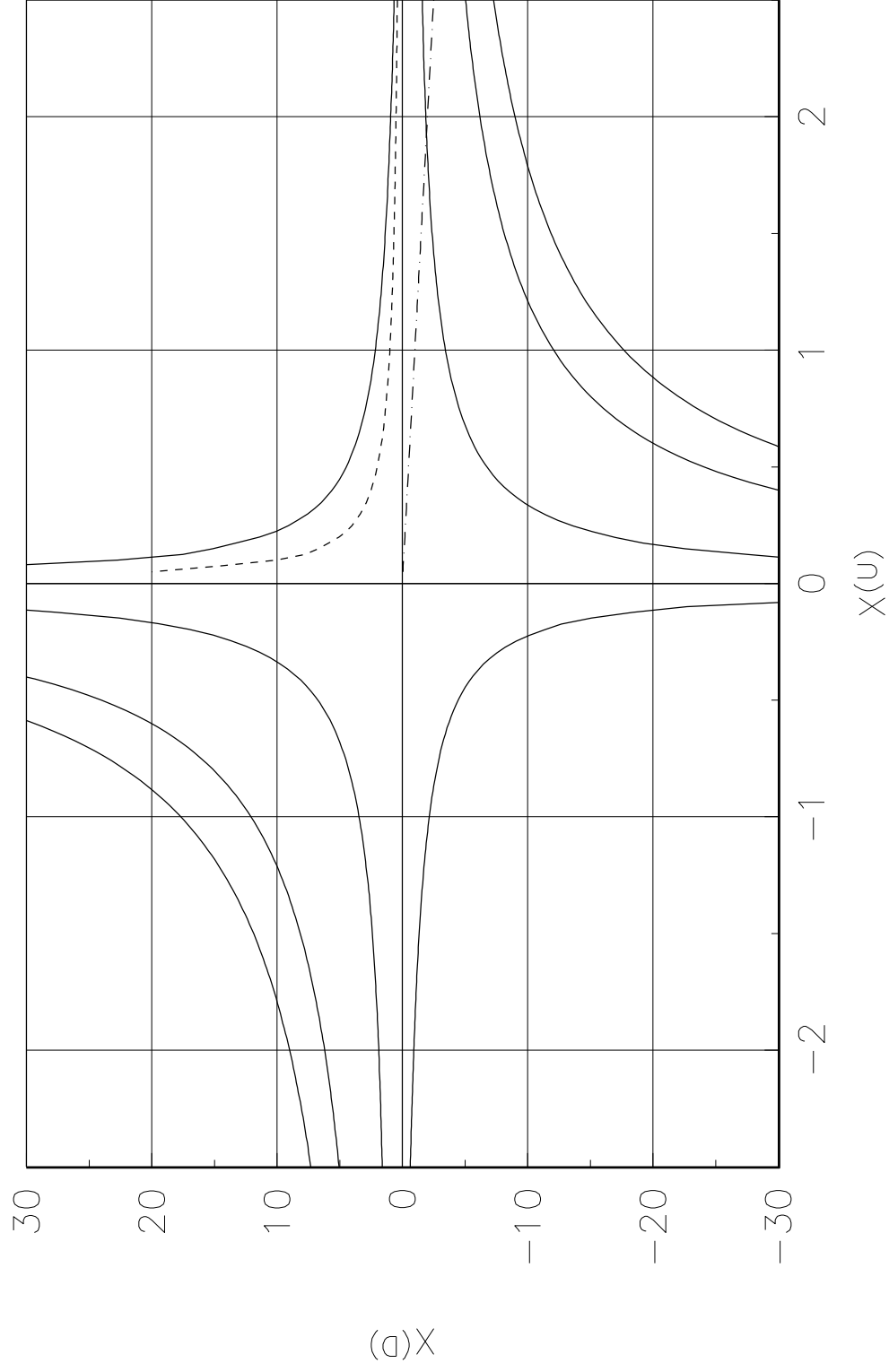


Fig. 3c: $M_{H^-} = 600$ GEV

